Comparative Study on Strain-Induced Crystallization Behavior of Peroxide Cross-Linked and Sulfur Cross-Linked Natural Rubber

Yuko Ikeda,*,† Yoritaka Yasuda,† Kensuke Hijikata,† Masatoshi Tosaka,‡ and Shinzo Kohjiya§

Graduate School of Science and Technology, Kyoto Institute of Technology, Matsugasaki, Sakyo, Kyoto 606−8585, Japan, Institute for Chemical Research, Kyoto University, Uji, Kyoto 611−0011, Japan, and Department of Chemistry, Faculty of Science, Mahidol University, Salaya Campus (SC4−303), Phuthamonthon, Nakorn Pathom 73170, Thailand

Received January 22, 2008; Revised Manuscript Received May 6, 2008

ABSTRACT: Strain-induced crystallization (SIC) behavior of natural rubber (NR) cross-linked by peroxide or sulfur was comparatively studied by time-resolved wide-angle X-ray diffraction measurements at SPring-8. Stretching ratio at the onset of SIC (α_c) decreased with an increase of network chain density (ν) for peroxide cross-linked NR (P-NR), while it remained constant for sulfur cross-linked NR (S-NR). But, dependence of relative crystallization rates on ν was similar for both P-NR and S-NR. Calculated entropy differences between the undeformed and the deformed states (ΔS_{def}) at α_c were equal for P-NR regardless of ν, whereas it became smaller with the increase of ν for S-NR. The SIC behavior of P-NR is in agreement with the prediction on homogeneous or uniform networks by Flory. Thus, the network structure of S-NR is supposed to be less homogeneous than that of P-NR. The inhomogeneity in S-NR is estimated due to the presence of domains of high ν value embedded in the rubbery network matrix, which is supported by the stress dependences of apparent lateral crystallite size. The mechanical characteristics of S-NR and P-NR are also discussed from the viewpoint of their SIC behaviors on the basis of the network structures.

Introduction

Natural rubber (NR) is standing alone among general-purpose rubbers: It is the only biomass among many commercially available rubbers and only one polymeric hydrocarbon among biopolymers. In addition, most of industrial "NR" originates from one species, *Hevea brasiliensis,* and the rubbery molecular chains in NR are highly stereoregular, i.e., composed of cis-1,4-isoprene units.[1] At room temperature, NR is amorphous under the quiescent condition, but highly crystallizable upon stretching. Nowadays, NR is of much necessity for many industrial and household applications.[2,3] Especially, NR is required for heavy-duty tires, essential components of vibration isolation structure against earthquakes, and medical products such as surgical gloves and condoms in thin film forms. In these applications, excellent tensile and dynamic mechanical properties of NR are important, together with its excellent crack growth resistance. These superior properties of NR have been assumed to be due to its strain-induced crystallization (SIC) ability.[2−5] Therefore, the study on SIC behavior of cross-linked NR is of utmost importance for elucidating the mechanical characteristics of NR.

Recent developments in computer technology and X-ray measurements at a synchrotron radiation source have enabled us to conduct time-resolved X-ray measurements during tensile deformation of soft materials. The advantage of using a synchrotron facility is to minimize relaxation effect by setting the irradiation time of X-ray on the sample much shorter than that of the conventional X-ray measurement. Consequently, structure−property relations of rubbery materials under tensile deformation have been revealed in real time, and several interesting results on SIC of NR and synthetic rubbers have been reported.[4−23] Among the synchrotron facilities now under operation, use of the beam lines at SPring-8[24] (Super Photon ring, 8 GeV) has given us further advantages to the dynamic study for structural analysis of soft matters.[4,16−19] For examples, we have managed to conduct SIC study by X-ray exposure time of 200 ms with 6 s interval.[18] Also, use of a high performance CCD camera has enabled us to conduct SIC studies during the fast stress relaxation process for sulfur cross-linked NR and isoprene rubber (IR), where the exposure time was set to 36 ms with the interval of 83 ms.[17,19] The results obtained under these extreme conditions showed that the rate of SIC of sulfur cross-linked NR (S-NR) was higher for the samples with the higher network chain density (ν), which is opposite to the trend reported in the former works conducted for the stretched samples under a small strain.[8,25] The differences may be ascribable to the difference in the time scale of wide-angle X-ray diffraction (WAXD) measurements. This example clearly suggests the importance of fast time-resolved X-ray measurements during deformation of rubber.

Up to now, most of the studies on SIC of cross-linked NR have been conducted on the S-NR samples,[4−15,17,20,26−33] which is due to the fact that the majority of NR products so far has been manufactured using the sulfur cross-linking system. Peroxide cross-linked NR (P-NR), however, is recently utilized more and more, owing to its high transparency (when not mixed with filler), lower compression set, and improved heat resistance. Thus, studies on SIC of P-NR, especially comparative studies on SIC of S-NR and P-NR, are important for development of future soft materials. However, there are only a few reports on the SIC of P-NR[6,12,16,29] including our rapid communication on a specific SIC behavior of P-NR.[18] There are no detailed comparative studies of S-NR and P-NR under the same experimental conditions on the basis of the time-resolved WAXD during a tensile deformation, as far as we know. During our study on SIC of P-NR at SPring-8, we found an interesting difference in the SIC behavior of P-NR compared to S-NR:[18] Stretching ratios at the onset of SIC (α_c) became smaller with the increase of ν for the P-NR. This result was different from our previous ones on S-NR,[10,13] where

* Corresponding author. E-mail: yuko@kit.ac.jp. Phone: +81 75 724 7558. Fax: +81 75 724 7580.
† Kyoto Institute of Technology.
‡ Kyoto University.
§ Mahidol University.

10.1021/ma800144u CCC: $40.75
Published on Web 07/01/2008

Table 1. Recipes and Network Chain Density of Cross-Linked NR Samples

sample code	P-NR-1	P-NR-2	P-NR-3	P-NR-4	S-NR-1	S-NR-2	S-NR-3
NR	100	100	100	100	100	100	100
DCP[a](phr[b])	1	2	2.5	3			
stearic acid					2	2	2
active ZnO					1	1	1
CBS[c]					1	1	3
sulfur					1.5	1.5	4.5
heat-pressing time[d] (min)	21	27	30	30	15	30	30
$\nu^e \times 10^4$ (mol cm^{-3})	0.76	1.38	1.70	1.93	1.02	1.32	1.83

[a] Dicumyl peroxide. [b] Part per hundred rubber by weight. [c] *N*-Cyclohexyl-2-benzothiazole sulfenamide. [d] Pressed at 155 and 140 °C for peroxide and sulfur cross-linking, respectively. [e] Network chain density determined on the basis of classical theory of rubber elasticity.

α_c values were equal among the samples of various ν. Is this distinct difference on α_c due to the different stretching speed or radiation time of X-ray? Is this ascribable to the overall differences in the chemical nature of cross-links in peroxide versus sulfur cross-linked elastomers? These questions have promoted us to conduct the present study.

In this paper, the characteristics of SIC for S-NR and P-NR are concurrently revealed by the fast time-resolved WAXD during stretching at SPring-8 under the same experimental conditions and discussed from the viewpoint of difference in the cross-linking system. The SIC behaviors of S-NR detected at the different synchrotron radiation facilities are also compared in order to elucidate a specific feature of S-NR. The revealed SIC behaviors are further related with its tensile properties. The results will be useful for the material design of rubber products.

Experimental Section

Materials. P-NR samples were prepared as follows. NR was mixed with dicumyl peroxide (DCP) on a two-roll mill. The mixtures were cross-linked by heat-pressing at 155 °C in a mold to give cross-linked NR sheets of 1 mm thickness. The recipes of NR mixtures and processing conditions are shown in Table 1. S-NR samples were also prepared by heat-pressing at 140 °C. The recipes of S-NR samples are shown in Table 1. The amounts of DCP and sulfur/accelerator were varied in order to change the network chain density (ν) of P-NR and S-NR, respectively. Ring-shaped specimens were cut out from the sheets, the inner and outer diameters of which were 11.7 and 13.7 mm, respectively. The ν values of samples were estimated from the results of tensile measurements using the equation of the classical theory of rubber elasticity.[27]

$$\sigma = \nu kT(\alpha - 1/\alpha^2) \tag{1}$$

where σ is stress, k is the Boltzmann constant, T is absolute temperature, and α is stretching ratio defined as $\alpha = l/l_0$, in which l_0 and l are the initial length and the length under deformation, respectively.

Simultaneous WAXD and Tensile Measurements. Synchrotron WAXD measurements were carried out at BL-40XU beam line of SPring-8 in Harima, Japan.[24] A custom-made tensile tester (ISUT-2201, Aiesu Giken Co., Kyoto) was situated on the beam line, and WAXD patterns were recorded during tensile measurement at room temperature (ca. 25 °C). The wavelength of the X-ray was 0.08322 nm and the camera length was 213 mm. The two-dimensional WAXD patterns were recorded using a CCD camera (HAMAMATSU C4880−50). Intensity of the incident X-ray was attenuated using a rotating slit equipped on the beam line, and the incident beam was exposed on the sample for 200 ms every 6 s. This exposure condition was selected in order to minimize a relaxation effect in the SIC evaluation and radiation damages to the specimens during the measurements. The absorption correction for thinning of the samples under stretching was carried out using calculated correction coefficients, which were estimated on the basis of absorption coefficients per density[34] and weight fractions of each element in the samples. Here, the affine deformation is assumed for all rubber samples on the basis of their measured Poisson's ratios, (for S-NR-1, S-NR-2, and S-NR-3, the measured values were 0.499, 0.496, and 0.498, respectively, and for P-NR-1, P-NR-2, P-NR-3, and P-NR-4 they were 0.495, 0.496, 0.497, and 0.495, respectively). Poisson's ratio was estimated on the basis of size measurements using a CCD camera (VC1000 Digital Fine Scope, OMRON Co.) during the tensile deformation. Intensities of the incident beam and transmitted beam through air were measured using ion chambers. The custom-made tensile tester enabled us to stretch the specimen symmetrically to examine the same position of the specimen by X-ray diffraction/scattering during the deformation. Ring-shaped samples were subjected to the tensile measurement in order to correctly measure the stretching ratio (α) of deformed samples. The stretching speed was 100 mm/min, i.e., strain speed was ca. 4.98/min.

WAXD Analysis. The obtained WAXD images were processed using "POLAR" (Stonybrook Technology & Applied Research, Inc.).[5,10,13] The WAXD patterns of stretched samples were decomposed into three components, i.e., isotropic, oriented amorphous, and crystalline components. Three components were azimuthally integrated within the range of ± 75° from the equator; the details of this analytical method were described in our previous paper.[13] Three structural parameters were estimated, of which "crystallinity index" (CI) and "oriented amorphous index" (OAI) are defined by the following equations, and "unoriented amorphous index" (UAI) is defined as UAI = 1 − (CI + OAI).

$$\mathrm{CI} = \frac{\sum_{\text{crystal}} 2\pi \int \sin\phi d\phi \int I(s)s^2 \mathrm{d}s}{\sum_{\text{total}} 2\pi \int \sin\phi d\phi \int I(s)s^2 \mathrm{d}s} \tag{2}$$

$$\mathrm{OAI} = \frac{\sum_{\text{oriented amorphous}} 2\pi \int \sin\phi d\phi \int I(s)s^2 \mathrm{d}s}{\sum_{\text{total}} 2\pi \int \sin\phi d\phi \int I(s)s^2 \mathrm{d}s} \tag{3}$$

In eqs 2 and 3, $I(s)$ represents the intensity distribution of each peak that is read out from the WAXD pattern, s is the radial coordinate in reciprocal space in nm^{-1} unit ($s = 2(\sin\theta/\lambda)$, where λ is the wavelength and 2θ is the scattering angle), and ϕ is the angle between the scattering vector of the peak and the fiber direction.

Coherent lengths (apparent crystallite sizes) were estimated by using the Scherrer equation (eq 4).[35,36]

$$L_{\mathrm{hkl}} = K\lambda/(\beta\cos\theta) \tag{4}$$

where L_{hkl} is the apparent crystallite size in the direction perpendicular to the (hkl) plane, and θ is the Bragg angle (half of the scattering angle). In this study, the value 0.89 was used for K[4,36] and β was determined as follows. The intensity distribution on the equator was extracted from the original WAXD pattern, and each peak was fitted with a linear background and a Gaussian function having the form $I(x) = h\exp[-(x - x_c)^2/(2w^2)]$, where $I(x)$ is the intensity at position x, x_c is the position at the scattering maximum, and h and w are parameters related to the peak height and peak width, respectively.[10] Each w value was converted into the half-width β.

Orientation fluctuations of 200 reflection were evaluated from azimuthal scan of the peak:[10] The width parameter in azimuthal

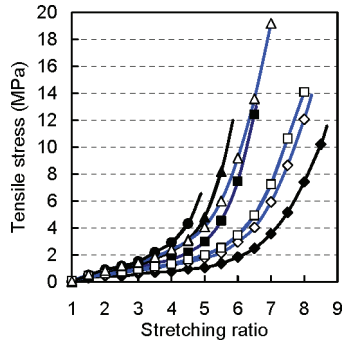

Figure 1. Tensile stress-strain curves of P-NR and S-NR samples: (filled diamonds) P-NR-1, (■) P-NR-2, (▲) P-NR-3, (●) P-NR-4, (open diamonds) S-NR-1, (□) S-NR-2, and (△) S-NR-3.

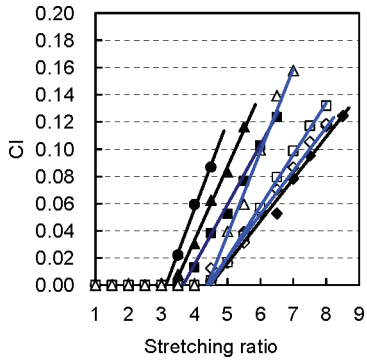

Figure 2. Relationship between crystallinity index (CI) and tensile strain of P-NR and S-NR samples: (filled diamonds) P-NR-1, (■) P-NR-2, (▲) P-NR-3, (●) P-NR-4, (open diamonds) S-NR-1, (□) S-NR-2, and (△) S-NR-3.

direction (w_{az}) was obtained by fitting the intensity distribution with a Gaussian function. Then, w_{az} was converted into half-width β_{az} by the following equation

$$\beta_{az} = 2w_{az}\sqrt{-2\ln(1/2)} \quad (5)$$

The lattice constants were estimated from each WAXD pattern during stretching using the least-squares regression method. The unit cell was approximated to be rectangular[37] for the easier treatment, which is reasonable as long as the discussion is limited to the mechanical response of the crystal.

The correction of instrumental broadening was not carried out in this study, due to the absence of zinc oxide crystallite in P-NR. (Zinc oxide was mixed only in S-NR as one of the components in sulfur cure system, see Table 1.)

Results and Discussion

Tensile Properties and Onset Strain of SIC. Figure 1 shows tensile stress−strain curves of the P-NR and S-NR samples, where the plotted points indicate the event of X-ray irradiation for the WAXD measurements. The stress−strain curves were displayed up to the mechanical rupture point of the samples. In correspondence to these tensile properties, variation of crystallinity index (CI) of all samples is shown against the stretching ratio (α) in Figure 2. For both P-NR and S-NR in Figure 1, the larger was the ν, the higher was the stress at any stretching ratio, and accordingly the steep upturn of stress at the intermediate strain region is observed at the lower strain. The slope after the upturn tended to become larger with the increase of ν in both P-NR and S-NR. Steep upturn of stress in tensile stress−strain curves has often been discussed on the basis of "speculated generation of crystals" upon stretching for crystallizable rubbers.[2,3,26] However, it may bring about a tricky or incorrect interpretation for soft materials. In fact, it was observed

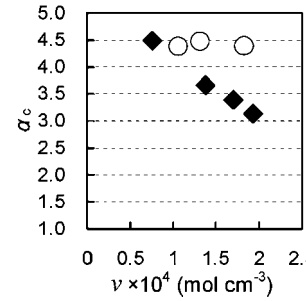

Figure 3. Effect of network chain density on onset strain of crystallization (α_c) of (filled diamonds) P-NR and (○) S-NR samples.

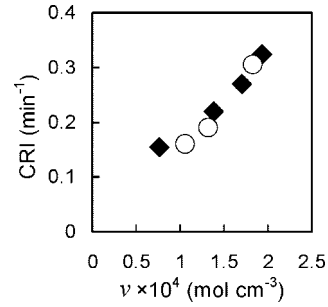

Figure 4. Effect of network chain density on crystallization rate index (CRI) of (filled diamonds) P-NR and (○) S-NR samples.

that a stretching ratio at which the crystallization started (α_c) was almost same among all S-NR samples, as shown in Figure 2, whereas their steep upturns of stress started at different strains. This feature has been also found irrespective of the compounding recipes of S-NR samples and/or experimental conditions of WAXD measurements during stretching.[8,10,13,38] On the contrary, α_c of the P-NR samples shifted to the smaller α for the samples with higher ν as shown in Figure 2, and accordingly, the steep upturn of stress occurred at lower strain as illustrated in Figure 1.[18] These results suggest that strain-induced crystallites do not always dominantly contribute to increasing the stress, but it depends on the samples. Thus, further studies on SIC of both peroxide and sulfur cross-linked NR samples are necessary in order to know the relationship between the tensile properties and SIC behavior for future material design of rubber products.

Here, it is noted that after the onset of SIC the crystallization linearly proceed with the strain as shown in Figure 2 and the present results on S-NR are different from those reported in our previous papers[10,13] obtained using dumbbell-shaped samples with the similar ν. The results there showed that the progress of SIC formed not linear but S-shaped curves. The difference may be ascribable to the slippage of a portion in the dumbbell-shaped rubber sample from the clamps at high strains. In fact, it was often observed that a portion of rubber came out from the clamps when the deformation was very large. This effect is damaging to the accurate determination of strain. Therefore, the use of the ring-shaped samples is much preferable for dynamical study of soft materials, and we believe that the present results on S-NR are more dependable for discussions.

Effect of Network Chain Density on Onset of SIC and Crystallization Rate. In order to quantitatively discuss the SIC behaviors of cross-linked NR, the effects of ν on the onset strain (α_c) and crystallization rate index (CRI) are plotted in Figures 3 and 4, respectively. CRI reflects a relative SIC rate and was obtained from the slope of linearly increasing line in Figure 2 as "CRI = (slope in the strain dependence of CI) × (strain speed)". The α_c values were determined by extrapolations of straight lines to x axis in Figure 2. As shown in Figure 3, dependence of α_c on ν for P-NR is clearly seen.[18] It agrees

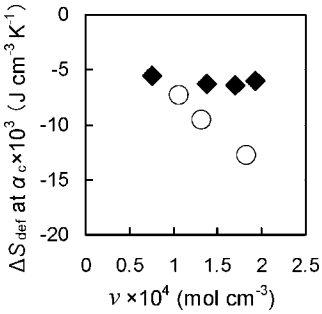

Figure 5. Effect of network chain density on ΔS_{def} at α_c of (filled diamonds) P-NR and (○) S-NR samples.

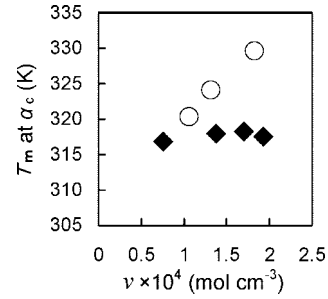

Figure 6. Effect of network chain density on T_m at α_c of (filled diamonds) P-NR and (○) S-NR samples.

well with the prediction by Flory[26,39] and is consistent with the classical theory of rubber elasticity.[27] For S-NR, however, the nondependence of α_c on ν is clearly observed by fast time-resolved WAXD/tensile measurements. This phenomenon is in accord with our previous result obtained under the stretching speed of 10 mm/min and X-ray irradiation time of 30 s at the simultaneous WAXD/tensile measurements on the dumbbell shaped samples, although the α_c values were ca. 3.2 (here ca. 4.4). The difference may be due to their different experimental conditions.[10,13] Therefore, in contrast to P-NR, the nondependence of α_c on ν for S-NR is concluded to be not in accordance with the classical theory of rubber elasticity,[27] and a specific feature of S-NR has to be elucidated.

On the other hand, it is interesting that CRI of both P-NR and S-NR shows almost the same ν dependence as shown in Figure 4. In our previous studies,[10,13,19,20] we proposed that the presence of extended network chains exceeding a certain length (at α_c) would be necessary for the NR samples to initiate SIC, which was found to be affected by cross-linking types, mentioned above. However, the same ν dependence of CRI for P-NR and for S-NR may imply that the SIC proceeds by the same mechanism in both samples not depending on the cross-linking types nor the difference of onset strain values, once the extended network chain is generated at α_c. Then, how to explain the constant α_c regardless of ν for S-NR? In order to elucidate this phenomenon, SIC behaviors of P-NR and S-NR are thermodynamically considered in the next section.

Effect of Network Chain Density on Entropy Difference between Undeformed and Deformed States at α_c. Entropy difference between the undeformed and the deformed states (ΔS_{def}) at α_c was estimated on the base of the classical rubber elasticity theory.[27] ΔS is entropy of fusion, $\Delta S_{def} = \Delta S_\alpha - \Delta S_1$, where the subscripts α and 1 stand for the stretching ratio at deformed and undeformed states, respectively. Under the assumption of affine deformation of Gaussian chains, ΔS_{def} is formulated by eq 6:

$$\Delta S_{def} = -(1/2)\nu k(\alpha_1^2 + \alpha_2^2 + \alpha_3^2 - 3) \quad (6)$$

where α_1, α_2, and α_3 are stretching ratios in the direction distinguished by the subscripts. When the Poisson's ratio of the sample is 0.5, eq 6 becomes

$$\Delta S_{def} = -(1/2)\nu k(\alpha^2 + 2/\alpha - 3) \quad (7)$$

Since the measured Poisson's ratios of samples were in the range of 0.495 − 0.499, eq 7 was reasonably applied to the samples. ΔS_{def} at α_c of all samples was calculated and is plotted against ν in Figure 5. The values of ΔS_{def} at α_c of the P-NR samples are almost equal in spite of their variation of ν, while those of the S-NR samples decreased (increased, in terms of absolute value) with the increase of ν. The result of P-NR implies that the SIC of P-NR occurred when a certain ΔS_{def} value was reached by stretching, regardless of their ν,[18] which is consistent with the fact that a chain elongated by the deformation depends only on the orientation of its end-to-end vector and not on its initial length.[26] However, this consideration is not applicable to S-NR. In S-NR, the larger the ν was the smaller the ΔS_{def} at α_c became. In other words, for the initiation of SIC, the larger was the ν the larger was also the length of stretched rubber molecules between the cross-linking sites.

Accordingly, the melting temperature at α_c ($T_{m,c}$) of strain-induced crystallites became higher with the increase of ν for S-NR, which was calculated using the obtained ΔS_{def} as follows. The melting temperature (T_m) in the deformed state is increased by an amount[31]

$$T_{m,\alpha} - T_{m,1} = (\Delta H_\alpha/\Delta S_\alpha) - (\Delta H_1/\Delta S_1) \quad (8)$$

If the heat of fusion (ΔH) is independent of the deformation ($\Delta H_1 = \Delta H_\alpha$), eq 8 is rewritten as

$$1/T_{m,\alpha} = (1/T_{m,1}) + (\Delta S_{def}/\Delta H_1) \quad (9)$$

For NR networks, it was reported that the heat of fusion was almost independent of deformation.[26] Therefore, eq 9 was used for the calculation of $T_{m,c}$, where $T_{m,1}$ and ΔH_1 were 308.5 K and 25.1 Jcm^3, respectively, per refs 40 and 41. Relationship between $T_{m,c}$ and ν is shown in Figure 6 for P-NR and S-NR. $T_{m,c}$ of strain-induced crystallites became higher with the increase of ν for S-NR, and those of P-NR were approximately constant and ca. 318 K regardless of their ν value.

Constant ΔS_{def} and $T_{m,c}$ of all P-NR samples with different ν studied here means that the supercooling at its onset of SIC is also constant regardless of ν. However, the supercooling at the onset of SIC of S-NR is dependent on its ν. These observations suggest that the network structures formed by peroxide and sulfur cross-linking should be different, because the SIC behavior of P-NR is in agreement with the prediction on homogeneous or uniform networks by Flory.[26,39] Thus, the network structure of S-NR is supposed to be less homogeneous when compared with that of P-NR. The next question then should be what kind of network structure was formed in S-NR.

Inhomogeneity of network structures in cross-linked rubbers has been known and actively discussed.[26,42] To mention two examples, the inhomogeneous network structures in sulfur-cured rubber vulcanizates were investigated by Fujimoto[43] as early as 1960s and by Vilgis et al.[44] Taking previous discussions into account, we propose here one probable heterogeneous network structure for S-NR, where domains of high ν are embedded in rubbery network matrix as shown in Figure 7. When cured by sulfur-accelerator system, two phases, i.e., A and B phases, in Figure 7 may be formed, where A and B stand for poor and rich phases, respectively, in terms of the density of cross-linking sites. In fact, sulfur is reported to be present near the surface of zinc oxide particle[45] and the sulfur cross-linking is active on the surface and/or around zinc oxide, which were confirmed by energy-filtering transmission electron microscopy.[46] These results are very supportive to our assumption of more inhomo-

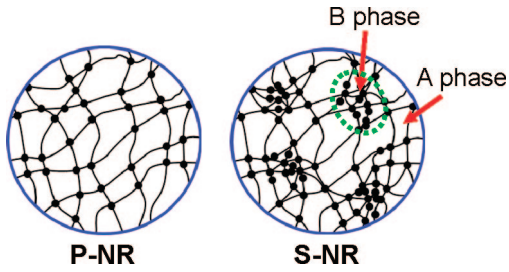

Figure 7. Speculated network morphologies of P-NR and S-NR.

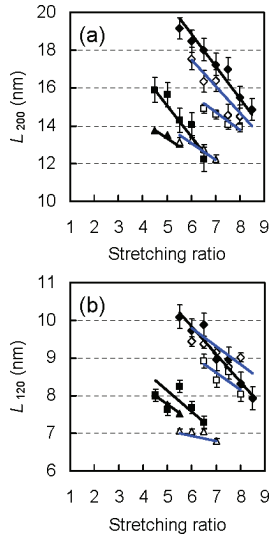

Figure 8. Relationships between apparent crystallite sizes and tensile strain of P-NR and S-NR samples: (a) L_{200}, (b) L_{120}; (filled diamonds) P-NR-1, (■) P-NR-2, (▲) P-NR-3, (open diamonds) S-NR-1, (□) S-NR-2, and (△) S-NR-3. The lines are guides for eyes.

geneous network structure in S-NR than P-NR. The domain of higher ν value can be ascribed to the result of the active sulfur cross-linking reactions due to the presence of sulfur around zinc oxide particles. In this study, B phase is termed as "network domain", because of its higher density of cross-linking points. Peroxide cure, on the other hand, affords more homogeneous random network structure relative to S-NR as shown in Figure 7. In order to investigate the relationship between the SIC behavior and the characteristic network structures of S-NR and P-NR, more detailed comparison of the strain-induced crystallites is discussed in the next section, where P-NR-4 was excluded due to its less data points.

Variation of Apparent Lateral Crystallite Sizes upon Stretching. For studying the crystallite growth dimensions by stretching, we estimated apparent crystallite size (coherent length) from WAXD profiles using the Scherrer equation.[35,36] The calculated coherent lengths are reasonably assumed to reflect an actual crystallite size at least in the *a*-axis direction. Figure 8a shows strain dependences of apparent lateral crystallite size estimated by using the 200 reflection (L_{200}) for all the samples. In the results of both P-NR and S-NR, the L_{200} value decreased with strain and L_{200} of the sample with larger ν was smaller even in the beginning of SIC. The variation of L_{200} by stretching (which corresponds to the slope of data points of each sample in Figure 8a) tended to be small in the sample with large ν for the both cross-linking systems. These phenomena were also detected in the plot of apparent lateral crystallite size estimated using the 120 reflection against the stretching ratio as shown in Figure 8b. The observation can be explained as follows: With the elongation of the sample, the number of stretched chains that can act as the initiating species for SIC

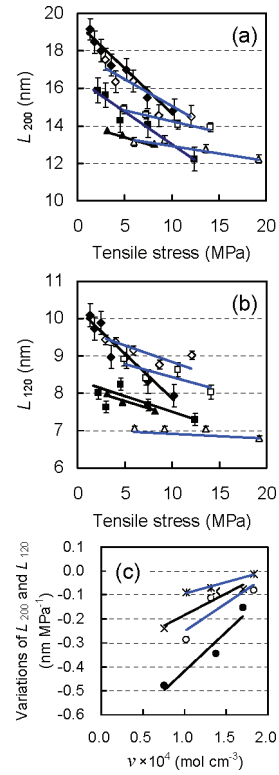

Figure 9. Relationships between apparent crystallite sizes and tensile stress of P-NR and S-NR samples: (a) L_{200}, (b) L_{120}; (filled diamonds) P-NR-1, (■) P-NR-2, (▲) P-NR-3, (open diamonds) S-NR-1, (□) S-NR-2, and (△) S-NR-3. Effect of network chain density on the variations of L_{200} and L_{120} by stress is shown in (c): (●) L_{200} of P-NR, (○) L_{200} of S-NR, (×) L_{120} of P-NR, and (∗) L_{120} of S-NR. The lines are guides for eyes.

must be increased. In the sample with the larger ν, the number of the initiating species is larger. However, the presence of cross-linking sites also hinders the development of SIC. The cross-linking sites are supposed to act as impurities or external entities during the crystallization of poly(isoprene) units in the rubber networks. As a result, the mean distance between the initiating species must decrease with the increase of ν and the average crystallite size should be also smaller. Upon further stretching, the generated crystallites also make a role as quasi-cross-linking sites and are followed by both promoting and hindering the SIC.

To the decrease of L_{200} and L_{120} values by further stretching, a rupture of generated crystallites must also have contributed. In addition, the crystallites are thought to be compressed by stretching from the lateral direction against the stretching direction, as discussed and explained in our previous paper using a pantograph-like model.[10,13] In fact, the effect of nominal stress on L_{200} is clearly detected as shown in Figure 9a. The sample with larger ν shows the smaller L_{200}, and the variation of L_{200} by the stress becomes smaller with the increase of ν under the defined stress for both P-NR and S-NR. The smaller variation of L_{200} by stress can be ascribable to the more loading of stress in the cross-linking sites than in the crystallites. It is worth noting that the variations of L_{200} by nominal stress became smaller in S-NR than in P-NR, as shown in Figure 9c, where the slopes in Figure 9a are plotted as the variations of L_{200} by stress against ν. This trend was also detected in the plot of L_{120} as shown in Figure 9b, although the slope was smaller than in the case of L_{200}. These observations suggest that the stress loading in the crystallites is smaller in S-NR than in P-NR, which must be ascribable to the specific feature of network structure in S-NR shown in Figure 7. When the two-phase network structure is subject to stretching, the stress is considered to be loaded on

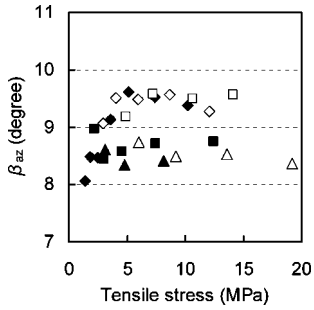

Figure 10. Relationship between β_{az} and tensile stress of P-NR and S-NR samples: (filled diamonds) P-NR-1, (■) P-NR-2, (▲) P-NR-3, (open diamonds) S-NR-1, (□) S-NR-2, and (△) S-NR-3.

both A and B phases. The network domains, B phases, are assumed to be loaded by the stress even after the onset of SIC. Therefore, the stress is considered to be less loaded by the strain-generated crystallites in S-NR than in P-NR, which would bring about the small variation of apparent lateral crystallite sizes by stretching for S-NR, as shown in Figure 9. This kind of discussions on the relationship between the heterogeneous network structure and dynamics of SIC behavior of cross-linked rubber have never been done, and the obtained results in this study may be the first of this kind.

Here, it should be kept in mind that the CRI of both P-NR and S-NR samples shows almost the same ν dependence as shown in Figure 4. The inhomogeneity of network structure influenced the apparent lateral crystallite sizes by stretching as shown above, but the development of crystallites in SIC was similar for all samples. These observations may bring about the following consideration: The inhomogeneity of network structure affects ΔS_{def} for initiating SIC. For an example, in S-NR, the presence of network domains decreased the ΔS_{def} at α_c with increase of ν, but it also decreased the loaded stress on the generated crystallites. SIC behavior upon stretching is involving two opposite processes: one is generation of crystallites and development of crystallites upon stretching, and the other is decrease in generation of crystallites and disappearance of generated crystallites. These phenomena are thought to randomly but more or less correlatively occur in rubber matrix. Therefore, the obtained results in this study imply that the inhomogeneity of network structure in cross-linked NR affects the development of these phenomena depending on its specific feature, but the crystallization rate in SIC is not related with the inhomogeneity of the network. It only depends on the overall network chain density of the samples regardless of the type of cross-linking. After the initiation of SIC, ΔS_{def} in a certain strain from one deformed state to the next deformed state is supposed to depend on the total network chain density of the samples and not on the network structure and the type of cross-linking. This consideration is consistent with eq 7. For generalizing these SIC phenomena, it is necessary to elucidate this point more on the other crystallizable rubbers.

Orientation Fluctuation of Crystallites by Nominal Stress. Figure 10 shows stress dependence of orientation fluctuation of crystallites for all samples. The obtained results were relative ones for the comparison of P-NR and S-NR in this study. There, the smaller value of β_{az} means the smaller fluctuations in orientation. As shown in Figure 10, it is observed that the larger the ν value the less the variation of orientation fluctuation by stress for both cross-linking systems. The results are in agreement with that of our previous study on S-NR,[10] and there is no distinct difference between P-NR and S-NR. The network domains in the matrix of S-NR are expected to decrease and increase the orientation of crystallites due to the steric hindrance and toughness at cross-linking sites, respectively. Therefore, the two opposite effects may cancel each other to result in a similar behavior of S-NR to that of the P-NR.

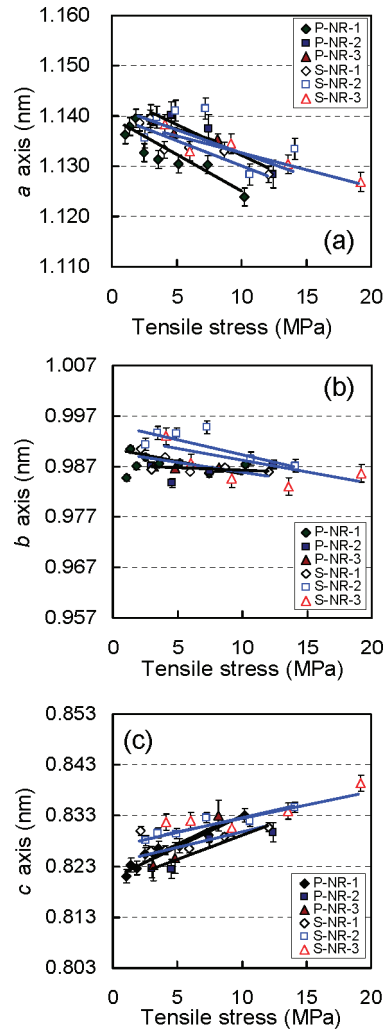

Figure 11. Relationships between lattice constants and tensile stress of P-NR and S-NR samples: (a) *a* axis, (b) *b* axis, and (c) *c* axis. The lines are guides for eyes.

Deformation of Crystal Lattice with Nominal Stress. Stress dependence of lattice constants of the strain-induced crystallites is shown in Figure 11. Despite the scatter of the values, there are apparent systematic trends for both S-NR and P-NR; the unit cell contracts along the *a* and *b* directions (perpendicular to the stretching direction) and elongates in the *c* direction (parallel to the stretching direction). The deformation of the unit cell approximately exhibits a linear relationship with the nominal stress in both S-NR and P-NR except the variation of *a* axis of S-NR-2. This result indicates that the strain-induced crystallites are responsible for the load in both cases. In addition, there is a difference in the variations of lattice constants by stress along the *a* and *c* directions between S-NR and P-NR; the slopes in the plots against stress of lattice constants tended to become smaller in S-NR than in P-NR. As discussed earlier, the network domains (B phase) in S-NR are supposed to load the stress even under the presence of crystallites by SIC. Thus, the smaller variation of lattice constants of *a* axis and *c* axis by stress in S-NR is also consistent with the proposed network structure of S-NR shown in Figure 7. On the variation of lattice constants along *b* direction, however, the effect of inhomogeneous structure was not consistently observed with that along *a* direction. The reason for this observation is not clear yet.

Onset of Crystallization for Sulfur Cross-Linked NR. As already described, the different SIC behavior between P-NR and S-NR may be understood on the basis of the inhomogeneity of the network structures of the samples, especially that of S-NR samples. However, this consideration does not directly suggest any reason for "the same onset strain of SIC for all S-NR samples". Thus, the formation of imhpmogeneous network structure in S-NR is next considered by taking the recipes for cross-linking NR into account. As shown in Table 1, several cross-linking reagents were mixed with NR for the preparation of S-NR with various ν values. The amounts of zinc oxide and stearic acid were same for all S-NR samples, whereas those of sulfur and accelerator (CBS) were varied. It is reported that stearic acid is reacted with zinc oxide to form zinc stearate, which accelerates the sulfur cross-linking.[47] In addition, sulfur is involved in the reaction with zinc oxide particle[45] together with CBS, and the sulfur cross-linking reaction is active on the surface and/or around zinc oxide, as mentioned in previous section. Since the same amounts of zinc oxide and stearic acid were used for all S-NR samples in this study, the products are assumed to have formed crystallizable chains of similar length in the matrix of S-NR (in A phase of Figure 7). The increase of ν on S-NR by increasing the heat-pressing time and the amounts of sulfur and accelerator may be due to the result of the more active sulfur cross-linking reactions around zinc oxide particles. (It is probable that ZnO was converted to ZnS after the reaction with sulfur. Thus, the particle may include ZnS.) These particles are possibly present in the B phase (the network domain), but this assumption has to be proved experimentally in a future. Therefore, the variation of sulfur content in the mixture is speculated to be more influential on formation of the network domains. The effective network chain length for SIC may be same among S-NR samples, which is in accord with our SIC results in this study.

Now, one may have an alternative explanation such as breaking and/or rearrangement of S−S bonds for the same onset strains of S-NR samples. However, the S-NR samples in this study were prepared according to the different recipes, where the amounts of sulfur and accelerator were varied and/or the heat-pressing time was different, as shown in Table 1. This means that the fractions of monosulfide, disulfide, and poly sulfide linkages may be different among the samples similar to a report[48] on the accelerated sulfur vulcanization, and consequently, the degrees of breaking and/or rearrangement of S−S bonds by stretching may not be same among the S-NR samples. Thus, it is difficult to ascribe the same onset strains of crystallization to this alternative explanation. Overall differences in the chemical nature of cross-links in peroxide versus sulfur cross-linked NR may be a factor. Our speculation of two phase network structure in S-NR has to be confirmed by a more specific analysis, if these chemical structures of the cross-links are influencing the two-phase structure. Small-angle neutron scattering experiments are now in progress, and more details on the heterogeneous network structure will be reported elsewhere.

Effect of SIC on Tensile Properties of Cross-Linked NR. Nowadays, S-NR is the most familiar type used in commercial rubber products; high performance rubber materials are generally produced by sulfur-cross-linking. In order to elucidate characteristics of tensile properties of S-NR, relationship between the SIC behavior and tensile properties of both S-NR and P-NR is discussed in this section. The tensile properties of S-NR are particularly focused from the viewpoint of the effect of specific domain in the networks (Phase B in Figure 7), because the onset strains of crystallization for all S-NR samples were almost same regardless of the value of ν. The tensile stress−strain curves of the samples are already shown in Figure 1. Corresponding to these tensile properties, the variations of unoriented amorphous index (UAI) and oriented amorphous index (OAI) of all samples are plotted against α in Figures 12 and 13, respectively. The lines in figures are drawn, referring polynomial fits for guidance to eyes, although the data of S-NR in Figure 13 are more

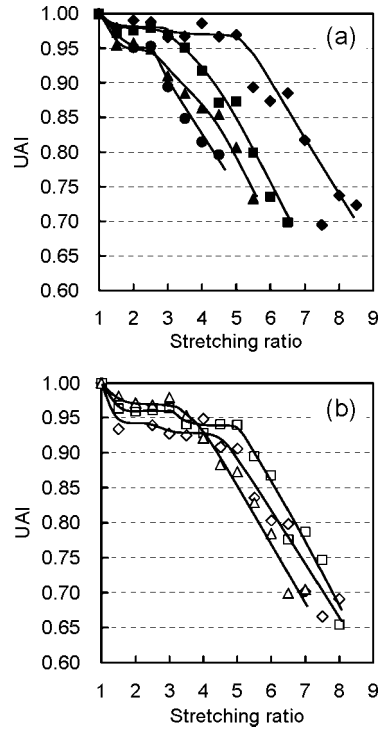

Figure 12. Relationship between unoriented amorphous index (UAI) and tensile strain of P-NR and S-NR samples: (a) P-NR,[18] (b) S-NR, (filled diamonds) P-NR-1, (■) P-NR-2, (▲) P-NR-3, (●) P-NR-4, (open diamonds) S-NR-1, (□) S-NR-2, and (△) S-NR-3. The lines are guides for eyes.

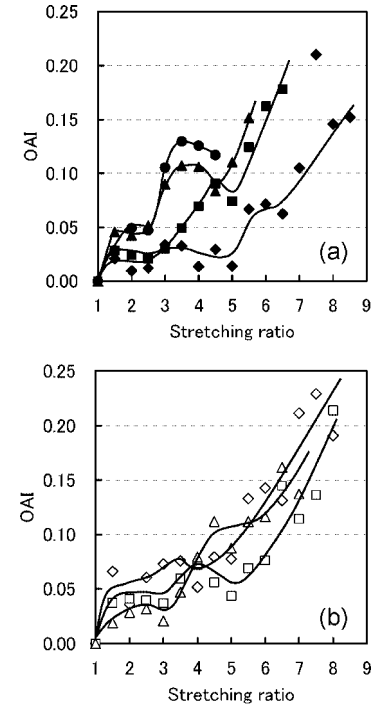

Figure 13. Relationship between oriented amorphous index (OAI) and strain of P-NR and S-NR samples: (a) P-NR,[18] (b) S-NR, (filled diamonds) P-NR-1, (■) P-NR-2, (▲) P-NR-3, (●) P-NR-4, (open diamonds) S-NR-1, (□) S-NR-2, and (△) S-NR-3. The lines are guides for eyes.

scattered compared to those of P-NR. By stretching, network chains immediately started orienting in the stretched direction, and consequently, UAI decreased as shown in Figure 12. The decrease of UAI for each sample tend to be slowing down after the initial stage, and UAI decreased again after a certain stretching ratio for both the cross-linked systems.

For P-NR, the second decrease of UAI shifted to the smaller strain with the increase of ν, which means that the orientation of rubber molecules by stretching is enhanced with the increase of ν. In addition, it is interesting that the inflection points seem to be correlated with α_c. There were, however, a large fraction of unoriented amorphous chains even at high strain for all P-NR samples, i.e., UAI was larger than or almost equal to 0.7 even at their highest strain of the P-NR samples with different ν values. In Figure 13, it was also observed that the OAI of each P-NR sample immediately increased by stretching, slowed down, and started increasing again gradually. After that, small decreases of OAI were observed for all P-NR samples followed by increase of OAI again with strain except for P-NR-4. On comparison of the variation of OAI with that of CI shown in Figure 2, the abrupt increase of OAI was found to be at the time of the onset of SIC. With the increase of ν, the increase of OAI became larger and the peak top of OAI tended to shift to the lower stretching ratio, at which point the definite strain for each sample was compared. On the relationship between tensile properties and SIC behavior of P-NR, it can be summarized that the larger the CI and OAI values are the higher the stress at low stretching ratio becomes. The SIC behavior of P-NR was found more or less to directly influence its tensile properties. These results are also useful in considering the tensile characteristics of S-NR.

Among the S-NR samples, the steep upturn of stress in S-NR-3 occurred at the lowest stretching ratio as shown in Figure 1. Before the onset of crystallization, however, the degree of orientation of rubbery network chains by stretching tended to become smaller with the increase of ν as shown in Figure 13, which is interestingly the opposite to the trend among the P-NR samples. This may be explained by our proposed network structure for S-NR shown in Figure 7. By stretching, for S-NR, molecular chains both in the network domains (B phases) and in the matrix phases (A phases) should be elongated. However, the orientation of the chains in the network domains in the stretching direction may become more and more difficult with the increase of cross-linking sites in the domains (accordingly with the increase of ν). Thus, OAI before the onset strain of SIC for S-NR-3 (the sample of the highest ν value) was the smallest among the S-NR samples, as shown in Figure 13, even though its stress remained to be the highest. For S-NR-3, it became clear that not only the strain-induced crystallites but also the oriented amorphous segments to the stretching direction did not contribute to its steep upturn of stress at the low strain before the crystallization. These results suggest that the network domains in rubbery matrix dominantly affect the tensile characteristics of S-NR before the onset of crystallization. At this stage, the network domains function like reinforcing fillers for rubber.

After the onset of crystallization in S-NR, the generated crystallites are supposed to be loaded with stress together with the network domains in S-NR. The OAI was found to become larger with the increase of ν when S-NR-2 and S-NR-3 were compared. Much more generated crystallites in S-NR-3 may have promoted the orientation of rubber molecules in the matrix. However, we should point out that OAI of S-NR-1 was still larger than that of S-NR-2. In the case of S-NR-1, by further stretching after the onset of crystallization, the rubbery chains in both A and B phases are supposed to orient in the stretching direction, due to the relatively low ν even in its network domains (B phase), to result in crystallization. The tensile strength of S-NR-1 shown in Figure 1 may be explained based on this characteristic.

Conclusion

A comparative study on the SIC behavior of P-NR and S-NR with various ν values was carried out by the fast time-resolved simultaneous WAXD and tensile measurements at SPring-8 using ring-shaped rubber samples. The results reveal us some important features of cross-linked NR not only on the network structure but also on the relationship of it with tensile properties.

For P-NR, it was observed that the onset strain of SIC (α_c) was smaller and the crystallization rate was faster for the samples with the larger ν values.[18] The entropy difference between undeformed and deformed states (ΔS_{def}) at α_c was nearly equal among the P-NR samples with different ν values. That is to say, SIC of P-NR occurred when the deformation reached a certain entropic state. These phenomena found in SIC of P-NR are in agreement with the prediction by Flory[26,39] and are consistent with the classical theory of rubber elasticity.[27] It was also observed that the larger the CI and OAI values, the higher is the stress at low stretching ratio, which suggests that the tensile properties are directly influenced by SIC of P-NR.

For S-NR, α_c was almost equal regardless of the values of ν in contrast with P-NR. Note that the S-NR samples were prepared according to the recipes of Table 1. The ΔS_{def} at α_c of S-NR became smaller with the increase of ν, which is also a different trend from P-NR. The observations on the SIC phenomena of S-NR were in conflict with the prediction by Flory,[27] which is based on the classical theory of rubber elasticity and on the assumption of uniform network structure. On the other hand, the crystallization rate increased with the increase of ν similarly to P-NR. Yet, the experimentally found phenomena are the characteristic feature of S-NR samples. Thus, the formation of less homogeneous network structure is proposed for S-NR, as shown in Figure 7; the domains of high network chain density are embedded in rubbery network matrix. This speculated morphology consistently explains the complicated phenomena observed in SIC of S-NR. The increases of CI and OAI did not dominantly contribute to the steep upturn of stress in S-NR, and the network domains in S-NR were responsible for loading the stress, especially before the onset of SIC. This network morphology was supported by the variations of apparent lateral crystallite sizes by nominal stress.

Up until now, many reports on the SIC behavior have been published, but most of the samples studied were sulfur cross-linked ones. Accordingly, more or less inconsistent results were obtained, which might be ascribed to the heterogeneous network structures originated from the sulfur cross-linking systems. Therefore, this study suggests that further investigations on the relationship between the network structure and SIC behavior of rubber materials prepared by various cross-linking methods become more and more important for scientific elucidation as well as technological developments on soft matters.

Acknowledgment. This work was partially supported by the Research Grants from President of KIT in 2004 and 2005 and the Ogasawara Foundation for the Promotion of Science & Engineering (to Y.I.). The authors want to express their thanks to Messrs H. Komori, K. Utani, Y. Kasahara, N. Yoshimura, S. Makino, and Dr. K. Senoo for their dedicated and useful assistance at SPring-8. The synchrotron radiation experiments were performed on BL-40XU line at the SPring-8 under the approval of the Japan Synchrotron Radiation Research Institute (Proposal No. 2003B0664-ND1b-np, 2005A0425-ND1b-np).

References and Notes

(1) Tanaka, Y. *Rubber Chem. Technol.* **2001**, *74*, 355–375.
(2) Mark,J. E. ; Erman,B. :Eirich,F. R. Eds. *Science and Technology of rubber, 2nd ed.* Academic Press, San Diego, 1994.
(3) Roberts, A. D. *Natural Rubber Science and Technology*; Oxford Science Publications: Oxford, 1988.
(4) Murakami, S.; Senoo, K.; Toki, S.; Kohjiya, S. *Polymer* **2002**, *43*, 2117–2120.
(5) Toki, S.; Sics, I.; Ran, S.; Liu, L.; Hsiao, B. S; Murakami, S.; Senoo, K.; Kohjiya, S *Macromolecules* **2002**, *35*, 6578–6584.
(6) Toki, S.; Sics, I.; Ran, S.; Liu, L.; Hasio, B. S. *Polymer* **2003**, *44*, 6003–6011.
(7) Toki, S.; Hsiao, B. S. *Macromolecules* **2003**, *36*, 5915–5917.
(8) Trabelsi, S.; Albouy, P. A.; Rault, J. *Macromolecules* **2003**, *36*, 7624–7639.
(9) Trabelsi, S.; Albouy, P. A.; Rault, J. *Rubber Chem. Technol.* **2004**, *77*, 303–316.
(10) Tosaka, M.; Murakami, S.; Poompradub, S.; Kohjiya, S.; Ikeda, Y.; Toki, S.; Sics, I.; Hsiao, B. S. *Macromolecules* **2004**, *37*, 3299–3309.
(11) Toki, S.; Sisc, I.; Hsiao, B. S.; Murakami, S.; Tosaka, M.; Poompradub, S.; Kohjiya, S.; Ikeda, Y. *J. Polym. Sci., Part B: Polym. Phys.* **2004**, *42*, 956–964.
(12) Toki, S.; Sisc, I.; Hsiao, B. S.; Murakami, S.; Tosaka, M.; Poompradub, S.; Kohjiya, S.; Ikeda, Y. *Rubber Chem. Technol.* **2004**, *77*, 317–335.
(13) Tosaka, M.; Kohjiya, S.; Murakami, S.; Poompradub, S.; Ikeda, Y.; Toki, S.; Sics, I.; Hsiao, B. S. *Rubber Chem. Technol.* **2004**, *77*, 711−723.
(14) Poompradub, S.; Tosaka, M.; Kohjiya, S.; Ikeda, Y.; Toki, S.; Sics, I.; Hsiao, B. S. *Chem. Lett.* **2004**, *33*, 220–221.
(15) Poompradub, S.; Tosaka, M.; Kohjiya, S.; Ikeda, Y.; Toki, S.; Sics, I.; Hsiao, B. S. *J. Appl. Phys.* **2005**, *97*, 103529/1–103529/9.
(16) Ikeda, Y. *Kauts.Gummi Kunstst.* **2005**, *58*, 455−460.
(17) Tosaka, M.; Kawakami, D.; Senoo, K.; Kohjiya, S.; Ikeda, Y.; Toki, S.; Hsiao, B. S. *Macromolecules* **2006**, *39*, 5100–5105.
(18) Ikeda, Y.; Yasuda, Y.; Makino, S.; Yamamoto, S.; Tosaka, M.; Senoo, K.; Kohjiya, S. *Polymer* **2007**, *48*, 1171–1175. Reprinted with permission of Elsevier.
(19) Tosaka, M.; Senoo, K.; Kohjiya, S.; Ikeda, Y. *J. Appl. Phys.* **2007**, *101*, 084909/1–084909/8.
(20) Kohjiya, S.; Tosaka, M.; Furutani, M.; Ikeda, Y.; Toki, S.; Hsiao, B. S. *Polymer* **2007**, *48*, 3801–3808.
(21) Ikeda, Y. *Kauts. Gummi Kunstst.* **2007**, *60*, 363–367.
(22) Ikeda, Y.; Kohjiya, S. *Nihon Reoroji Gakkaishi* **2008**, *36*, 9–17.
(23) Tosaka, M. *Polym. J.* **2007**, *39*, 1207–1220.
(24) http://www.spring8.or.jp/j/.
(25) Gent, A. N. *Trans. Faraday Soc.* **1954**, *50*, 521–533.
(26) Flory, P. J. *Principles of polymer chemistry*; Cornell University: Ithaca, New York, 1953.
(27) TreloarL. R. G. *The physics of rubber elasticity*; Clarendon Press: Oxford, 1975.
(28) Mandelkern, L. In *Crystallization of Polymers*, 2nd ed.; Cambridge University Press: Cambridge, 2004, *Vol.2.*
(29) Smith, J. Jr.; Greener, A.; Ciferri, A. *Kolloid Z.* **1964**, *194*, 49–67.
(30) Mitchell, J. C.; Meier, D. J. *J. Polym. Sci., Part A-2* **1968**, *6*, 1689–1703.
(31) Yamamoto, M.; White, J. L. *J. Polym. Sci., Part A-2* **1971**, *9*, 1399–1415.
(32) Luch, D.; Yeh, G. S. Y. *J. Macromol. Sci.* **1973**, *7*, 121−155.
(33) Toki, S.; Fujimaki, T.; Okuyama, M. *Polymer* **2000**, *41*, 5423–5429.
(34) HahnT. *International Tables for Crystallography*; D. Reidel Pub. Co.: Holland, 1983; *Vol. A*, p 157.
(35) Scherrer, P. *Göttinger Nachrichten* **1918**, *2*, 98. *Nachr. Ges. Wiss. Göttingen*, **1918**, 96–100.
(36) Klug, H. P.; Alexander, L. E. In *X-ray Diffraction Procedures for Polycrystalline and Amorphous Materials, 2nd ed.*; Wiley-Interscience: New York, 1974; p 687.
(37) Nyburg, S. C. *Acta Crystallogr.* **1954**, *7*, 385–392.
(38) Chenal, J.-M.; Chazeau, L.; Guy, L.; Bomal, Y.; Gauthier, C. *Polymer* **2007**, *48*, 1042–1046.
(39) Flory, J. P. *J. Chem. Phys.* **1947**, *15*, 397–408.
(40) Dalal, E. N.; Taylor, K. D.; Phillips, P. J. *Polymer* **1983**, *24*, 1623–1630.
(41) Kim, H. G.; Mandelkern, L. *J. Polym. Sci., Part A-2* **1972**, *10*, 1125–1133.
(42) Erman, B.; Mark, J. E. *Structure and properties of rubberlike networks*; Oxford Univ. Press: Oxford, 1997.
(43) Fujimoto, K. *Nippon Gomu Kyokaishi* **1964**, *37*, 602–619.
(44) Vilgis, T. A.; Heinrich, G. *Kautschuk Gummi Kunstst.* **1992**, *45*, 1006–1014.
(45) Steudel, R.; Steudel, Y. *Chem. Eur. J.* **2006**, *12*, 8589−8602.
(46) Horiuchi, S.; Dohi, H. *Langmuir* **2006**, *22*, 4607–4613.
(47) Hummel, K.; Santos Rodoriguez, F. J. *Kautsch. Gummi Kunstst.* **2001**, *54*, 122–126.
(48) Bateman, L. *The chemistry and physics of rubber-like substances*; Maclaren & Sons: London, 1963; pp 449−561.

MA800144U